Theoretical Chemistry Accounts (2020) 139:132
https://doi.org/10.1007/s00214-020-02646-4

REGULAR ARTICLE

Molecular modeling of MCPA herbicide adsorption by goethite (110) surface in dependence of pH

Ivelina Georgieva[1] · **Michael Kersten**[2] · **Daniel Tunega**[3,4]

Received: 12 March 2020 / Accepted: 2 July 2020 / Published online: 17 July 2020

Abstract

The sorption mechanism between 4-chloro-2-methylphenoxyacetic acid (MCPA) herbicide and the dominating (110) surface of the mineral goethite was studied by molecular modeling of the full set of possible surface complexes using density functional theory with periodic boundary conditions for the structural surface models. The most stable arrangements of the MCPA species were predicted taking into account the type and topology of the surface OH groups, protonation states (pH effect), the structure of carboxyl/carboxylate group of MCPA, and the binding type (outer- or inner-sphere complexes). Acid–base properties of MCPA and the goethite surface OH groups led to creation of several pH ranges (3–4, 4–9, 9) for combining neutral/deprotonated MCPA with neutral/protonated goethite surface. The predicted strongest adsorption (physisorption) for the complexes in the pH 4–9 range was followed by largest solvent destabilization of the outer-sphere complexes due to the high solvent energy of the MCPA and surface hydration of the hydroxylated goethite surface. In line with experimental data, the adsorption of MCPA should increase with decreasing pH owing to the presence of neutral MCPA molecule ($pK_a \sim 3$) and its lower solvation energy that can produce more stable complexes in solution than that of anionic MCPA in pH 4–9 range. The formation of the inner-sphere chemisorbed surface complex contributes significantly to the overall adsorption of MCPA at acidic pH range. In the chemisorbed inner-sphere complexes, monodentate binding was revealed through the formation of a Fe–O–C bridge.

Keywords Environmental pollution · Density functional theory · Goethite · MCPA herbicide

1 Introduction

Phenoxyalkanoic acids represent a base for a broad spectrum of modern herbicides extensively used in agriculture. They reduce the spread of broadleaved weeds on land and hence protect the cereals and vineyards. Because of a potential risk of contamination of groundwater sources [1], it is important to trace and understand the fate and behavior of herbicides after their release into environment until their final mineralization in soil. These herbicides contain one or more polar carboxylic groups responsible for their relatively high chemical reactivity with soil components. The physical and chemical processes of phenoxyacetic acid-based herbicides in soils and/or soil components (solubility, adsorption–desorption, chemical resistance, bio-, and photodegradation) were extensively investigated by a variety of experiments [2–16]. A strong dependence of the adsorbed amount on pH and on the presence of electrolytes in solution was observed [12, 13, 17]. The mobility and fixation of herbicides in soils are determined mainly by adsorption–desorption processes,

"Festschrift in honor of Prof. Fernando R. Ornellas" Guest Edited by Adélia Justino Aguiar Aquino, Antonio Gustavo Sampaio de Oliveira Filho and Francisco Bolivar Correto Machado.

Electronic supplementary material The online version of this article (https://doi.org/10.1007/s00214-020-02646-4) contains supplementary material, which is available to authorized users.

✉ Ivelina Georgieva
ivelina@svr.igic.bas.bg

✉ Daniel Tunega
daniel.tunega@boku.ac.at

[1] Institute of General and Inorganic Chemistry, Bulgarian Academy of Sciences, "Acad. G. Bonchev" Str. bld. 11, 1113 Sofia, Bulgaria

[2] Geosciences Institute, Johannes Gutenberg University, Becherweg 21, 55099 Mainz, Germany

[3] Institute of Soil Research, University of Natural Resources and Life Sciences, Peter-Jordan-Str. 82, 1190 Vienna, Austria

[4] School of Pharmaceutical Science and Technology, Tianjin University, Tianjin 300072, People's Republic of China

which can vary with amount, distribution, and properties of soil constituents, and with the chemical properties of herbicides. Significant relationships have also been found between adsorption and mineralization rate of these chemicals in soil [18]. Experiments describe in most cases sorption from aqueous solutions to mixed solid matrixes and provide mainly a global view on the interactions of pollutants in soil in a form of the soil-solution distribution coefficient, K_d. Only rarely, adsorption energies or enthalpies are calculated from fits to experimental data. Detailed, molecular scale characterization of mechanisms of interactions of these pollutants with soils or soil components is difficult to achieve from the experiment or spectroscopic data. In this context, methods of molecular modeling represent an effective tool to obtain details how pollutants interact with soil matrices. These methods have been successfully applied to predict interaction type and interaction energies of phenoxyacetic acid-based herbicides and polycyclic aromatic hydrocarbons with the soil components [19–23].

Among the soil minerals known as potential geosorbents for polar herbicides, the iron oxyhydroxides (FeOOH) manifest the highest herbicide partition coefficient (K_d value) [24]. Hence, they appear as best sorbents for phenoxy acid herbicides thanks to their high point of zero charge (pH_{PZC}). Moreover, iron oxyhydroxides contribute to large specific surface areas of soils, even though they are present in relatively low amounts in bulk soils [25]. Goethite (G), α-FeOOH, is a common oxyhydroxide mineral in many soils, and its sorption properties are related to the surface structure and nanoparticle grain size [26–29]. An experimental study has shown that humic matter coating the iron oxyhydroxides in soil only slightly changed their sorption capacities for phenoxy herbicides at ambient soil pH values [26]. The interaction mechanism of adsorption of phenoxyacetic acids to Fe-oxyhydroxide surfaces is still not fully clear, which warrants further investigations.

Clearly, the acid–base properties of the goethite surface hydroxyl groups and MCPA are a key to understand their interaction depending on pH of the environment. For bulk goethite, the experimental pH_{PZC} values are in a range of 7.5–9.5 depending on the amount of carbonate adsorbed [30], indicating an overall base character of the goethite surface. However, the proton affinity constants, pK_a, for individual types of surface OH sites cannot be obtained experimentally. The adsorption isotherms of MCPA on goethite have shown that the amount of adsorbed MCPA decreases with an increase of the pH of the medium from 3 to ~ 7, and with an increase of the MCPA concentration [23, 26, 31]. In the previous studies, the adsorption isotherms at pH 4 and pH 7 were interpreted in terms of the formation of electrostatic forces between MCPA anion and protonated goethite [26, 31, 32]. The linear decrease in MCPA adsorption with increasing pH values was explained simply by decrease in the positive surface charge of the goethite. At the same time, the observed decrease in MCPA adsorption with increase in ionic strength at pH 4 (electrolyte KCl) was an additional argument for outer-sphere complex formation [26]. In other studies, adsorption isotherms for phenoxy acid herbicides have been explained by a formation of monodentate or bidentate inner-sphere surface complexes on Fe oxyhydroxides, but this has been claimed without evidence by spectroscopic or molecular modeling methods [25, 26, 32]. FTIR spectra of adsorbed phenoxy acid herbicides also did not provide unambiguous confirmation about the mechanism of binding. In fact, the measured spectra were quite complex and difficult to interpret with overlapping low-intensity bands in the region of interest [33]. Recent studies (using electrolyte $NaNO_3$) have shown that ionic strength of the background electrolyte did not affect the adsorption results significantly in the acidic pH range [23]. Similarly, the consistent results were found for the adsorption of a phenoxy acid herbicide to Fe oxyhydroxides at different background electrolyte concentrations of $CaCl_2$. This result indicated that the adsorption of MCPA by the protonated goethite surface was likely dominated by inner-sphere complexation of the neutral molecule. Adsorption isotherms of MCPA-goethite at pH 3–6 have shown that the maximum adsorption was even below the MCPA pK_a value [23]. This result leads to the conclusion that the interactions between MCPA and goethite depend on the speciation of the adsorbate rather than being electrostatically controlled (as it has been previously suggested [26]). Hence, the decrease in the fraction of MCPA adsorbed by goethite coated with humic acid relative to pure goethite has been explained with the effect of the organic coating to decrease the number of reactive surface sites available to interact with the MCPA molecules rather than with the electrostatic effects like changes in the goethite surface pH_{PZC} [23, 26]. At highly acidic (pH < 3) goethite dissolves, which hampers the adsorption studies below the MCPA pK_a (3.07) [23]. In basic solution (pH > 9), surface μ-OH groups (pK_a ~ 9–10) become deprotonated, $FeOH_2^+$ sites (pK_a ~ 12) neutralized to FeOH [34], and MCPA is in anionic form. Therefore, adsorption is hampered by electrostatic repulsion, which could explain the strong decrease in MCPA adsorption observed with increasing pH.

The charge distribution multisite complexation model (CD-MUSIC) has been used to describe the binding type of the MCPA to the goethite on a macroscopic level [23, 26]. Structural information necessary for a sound CD-MUSIC modeling was derived from first principle molecular dynamics (FPMD) performed on two hydrated models of MCPA-goethite complexes in our previous study. In this way, a decrease in the number of adjustable CD-MUSIC model parameters has been achieved, allowing the adsorption model constants for the most probable inner-sphere and outer-sphere surface complex structures to be unequivocally

determined. The adsorption constants for the complexes were successfully fitted to experimental batch equilibrium data, and the adsorption isotherms were interpreted in terms of formation of monodentate inner-sphere surface complexes of neutral MCPA on partially protonated goethite surface reflecting pH_{50} below 4 (adsorption edge) [23].

The present work reports detailed discussion on explanation of surface complexation of MCPA on the most populate goethite surface (110) using the full set of possible complexes and applying the density functional theory (DFT) method. The focus of this study is to look in more detail at (1) all possible sorption mechanisms, (2) the role of different surface hydroxyl groups, and (3) the pH effect on the form and stability of the surface complexes. The aim is thus to predict the most stable arrangements of the MCPA species taking into account typical characteristics such as complex surface topology of the surface OH groups (–OH, –μOH, and $–\mu_3$OH), protonation states (pH effect), and binding types (outer- or inner-sphere complexation). The MCPA-goethite complexes are characterized by means of energy calculations for a variety of possible model systems (MCPA-goethite interaction energy), detailed geometry characterization of the surface goethite Fe–O bonds, and adsorbed MCPA hydrogen bonds (HB).

2 Structural and computational details

The interactions of MCPA, both in neutral and anionic molecular form, with the dominating goethite surface (110) were modeled using the periodic plane-wave DFT approach. The electronic structure calculations were performed using the Vienna ab initio simulation package VASP [35] using a spin-polarized DFT formalism. Electron exchange–correlation interactions were treated using the generalized gradient approximation (GGA) as parameterized by Perdew, Burke, and Ernzerhof (PBE functional) [36]. The Kohn–Sham equations were solved variationally in a plane-wave (PW) basis set with an energy cutoff of 400 eV. The electron–ion interactions were described using the projector-augmented-wave (PAW) method [37]. Fourteen valence electrons for each Fe atom ($3p^6 3d^7 4s^1$), six valence electrons for each O atom ($2s^2 2p^4$), four valence electrons for each C atom ($2s^2 p^2$), and seven valence electrons for each Cl atom ($2s^2 p^5$) were treated explicitly, and the remaining core electrons and the nuclei were described by PAW pseudopotentials.

Goethite has strongly correlated *d*-electrons, so the DFT + *U* approach worked out by Dudarev et al. [38] was used in all calculations to describe the strong Coulomb repulsion (*U*) between the localized *d* electrons in the Fe. In the DFT + *U* framework, a Hubbard-like term to the effective potential is added to improve description of correlation effects in transition metal oxides. The effective Hubbard parameter $U_{\text{eff}} = U - J$ enters the Hamiltonian, with *J* being the exchange interaction parameter. The effective on-site Coulomb and exchange interaction parameters for each iron atom were set to 4 eV and 1 eV, respectively, as used in a previous study of the bulk structure of goethite [20].

Quantum chemical electronic structure calculations for iron oxides account for 3*d* electrons in open-shell formalism. Spin-crossover coupling exists between iron centers in structures such as of goethite. Several theoretical studies on the bulk structure of goethite showed that the high spin antiferromagnetic (AFM) configuration ($2S + 1 = 6$, where *S* is a spin number) has been found as the most stable magnetic structure [39, 40]. Thus, this high spin AFM configuration was also used for a slab model of the dominant (110) surface, similar to a previous study of the adsorption of polycyclic aromatic hydrocarbons by goethite [20]. The slab was derived from the experimental bulk structure ([41], *Pbnm* space group) with a thickness ~ 9 Å having in total 114 atoms (24 Fe, 54 O and 36 H). The computational cell was orthorhombic with lateral cell vectors $b = 11.0$ Å and $c = 9.1$ Å. In the *a*-direction, a vacuum of ~ 21 Å was added getting a total *a* vector of 30.0 Å. Oxygen atoms of broken Fe–O bonds on the upper and lower surfaces of the slab were saturated by hydrogen atoms to get the slab electrostatically neutral. The (110) surface is formed by three types of surface hydroxyl groups, particularly (1) hydroxo sites (OH groups bound to one iron atom), (2) μ-hydroxo sites (μOH groups connected to two iron atoms), and μ_3-hydroxo (μ_3OH, where the oxygen atom is bound to three iron atoms). This structural arrangement is depicted in Fig. 1b.

Surface complexation models were constructed by inserting the MCPA molecule or anion near the surface hydroxyl groups considering both outer- and inner-sphere complexation on the goethite surface. The sixfold coordination of Fe does not change upon complexation including chemically bound MCPA. The complex structure of the surface (topology of three different OH groups) and the structure of adsorbate (two sites for binding through carboxyl/carboxylate groups, Fig. 1a) offer a variety of surface complexes being considered. Moreover, in order to cover a broad range of pH in the calculations, it was also necessary to consider protonation and deprotonation states of the MCPA molecule and the surface OH groups. All these factors gave a plenty of options for binding of MCPA to the surface. In total, 25 models were thus constructed (Table 1).

Structural optimizations of all models have been performed with the optimization engine GADGET [42] based on delocalized internal coordinates [43]. All of the atomic positions were fully relaxed without symmetry restrictions by keeping fixed unit cell parameters. The structures were relaxed when all components of the gradient vector were smaller than 4×10^{-4} atomic units. Only Γ-point sampling was used to integrate over the Brillouin zone, because

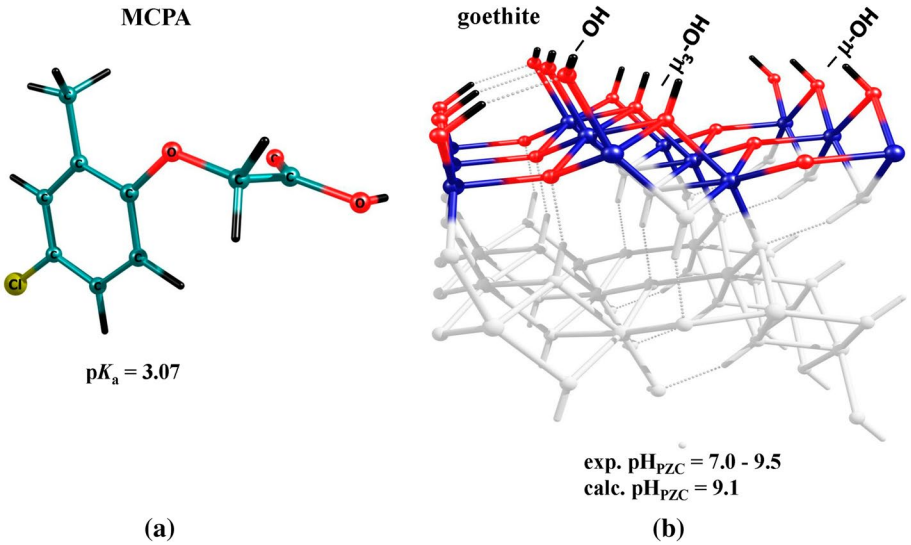

Fig. 1 **a** MCPA structure and **b** surface OH groups in 2D periodic (110) slab model of goethite—hydroxo sites (OH) (an oxygen atom bound to one iron atom), μ-hydroxo sites (μ-OH) (an oxygen atom bound to two iron atoms), and μ_3-hydroxo (μ_3-OH) (an oxygen atom bound to three iron atoms). For details on experimental and calculated pH$_{PZC}$, see Refs. [30, 34]

Table 1 Number of model configurations for MCPA-goethite complexes for different pH ranges

pH	3–4	4–9	4–9	> 9
MCPA	Neutral	Anion	Neutral (hypothetical)	Anion
Goethite	$-OH_2^+$	$-OH_2^+$	–OH	–OH
	μOH	μOH	μOH	μOH
	μ_3OH	μ_3OH	μ_3OH	μ_3OH
Outer-sphere complexes (physisorption)	2	3	6	6
Inner-sphere complexes (chemisorption)	3	2	3	

the computational cell was satisfactorily large. When the relaxed structures were obtained, relative energetic stabilities of the resulting configurations were compared for similar types of the complexes. Further, calculated interaction (reaction) energies were obtained in a following manner. Formally, a formation of physisorbed (outer-sphere complexes) can be considered as association reaction $A + B \rightarrow C$ and corresponding interaction energy is calculated as $\Delta E_{int} = E(C) - (E(A) + E(B))$. Formation of chemisorbed (inner-sphere complexes) is a reaction of exchange type $A + B \rightarrow C + D$, and reaction (interaction) energy is obtained as $\Delta E_{int} = (E(C) + E(D)) - (E(A) + E(B))$. In all cases, the total electronic energies E(A), E(B), E(C), and E(D) are taken for all fully optimized species involved in the reactions. The calculated interaction (reaction) energies did not contain contributions by zero-point vibrational energy, thermal corrections, and entropy effects.

The strengths of the surface Fe–O bonds in goethite and their changes upon complexation, i.e., physi- and chemisorption of MCPA, were evaluated by the bond-order (BO) analysis based on the density-derived electrostatic and chemical (DDEC6) method using an effective all-electron density [44] from VASP calculations. The DDEC6 method, implemented in the CHARGEMOL software [45], served as a practical definition of bond order across diverse materials in solid state [46, 47]. The BO index is defined as the number of electrons exchanged between a pair of atoms. Eventually, in the molecular orbital theory, BO is defined as half the difference between the number of bonding and antibonding electrons.

3 Results and discussion

3.1 MCPA-goethite models

The possible MCPA-goethite complexes at different pH were modeled on the basis of their acid–base properties. Below a pH$_{PZC}$ = 9.1, protonated OH sites of the goethite surface were assumed. According to the calculated pK_a values for the proton affinity reaction ($S\text{-}OH_2^+ \rightarrow S\text{-}OH + H^+$) for the three surface OH types, only –OH (hydroxo) sites could be protonated [34]. Our periodic slab model has a row of three –OH groups that are the only candidates for protonation. However, it was not possible to protonate all –OH groups because of extreme polarization and electrostatic repulsion effects among all three protonated OH sites that led to structural instability during the geometry optimization. Therefore, the surface protonation was simulated by adding one proton to one –OH group from the row to mimic a partially protonated surface below pH$_{PZC}$.

Depending on a pH range, neutral or deprotonated MCPA species are anticipated to adsorb on protonated or neutral goethite surface. Neutral MCPA molecule can interact

through the carbonyl oxygen and/or OH group of the carboxyl group (–COOH). The anionic MCPA form has two oxygen atoms of the carboxylate group available for the interaction. Existence of active sites of the (110) goethite surface ($–OH_2^+$, –OH, –μOH, $–μ_3OH$) allows a variety of surface complexes (Fig. 1). Two basic mechanisms are suggested for adsorption of MCPA, which are (1) physisorption with a formation of an outer-sphere complex, or (2) chemisorption with a formation of an inner-sphere complex [26]. In the outer-sphere type, MCPA interacts with the goethite surface via hydrogen bonding and/or other non-bonding interactions (e.g., electrostatic). Apart from physisorption, inner-sphere complexes can be formed during the chemical reaction of the surface like dehydroxylation and the water elimination with MCPA binding directly via ligand exchange to Fe in mono- or bidentate forms. It is not expected that $μ_3OH$ groups are involved in this process as the bond breaking of three Fe–O bonds would be energetically too consumable. Therefore, in our calculations, only OH and μOH groups were taken into account. Considering all above-mentioned factors, we categorized our models into three pH range groups—pH ~ 3–4, pH 4–9, and pH > 9—taking into account the different protonation states of MCPA and the goethite surface (Table 1). This categorization also includes a group of hypothetical complexes for a pH range 4–9 represented by neutral MCPA molecule and neutral goethite surface. Specific interactions between chlorine atom of the aromatic ring and surface hydroxyl groups were also detected in the optimized geometries that could contribute to the overall stability of the surface complexes. The existence of this interaction was attributed to the flexibility of the torsional C–C-O-C angle of MCPA. A compilation of the calculated relative electronic energies and the reaction energies for the relaxed equilibrium structures is presented in Table 2 and discussed in following chapters.

Table 2 Calculated relative electronic energies ($ΔE_{rel}$) and interaction (reaction) energies ($ΔE_{int}$) for complexes of MCPA formed on the (110) surface of goethite

Models[a]	$ΔE_{rel}$ Δ	$ΔE_{int}$
Physisorption **pH ~ 3–4**		
nos-pg-OH_2^+-OH	0.0	– 81.2
nos-pg-OH_2^+-μOH	13.8	– 69.5
Chemisorption		
nis-pg-md-OH_2^+(OH)	0.0	– 102.5 PT
nis-pg-md-OH_2^+(μOH)	82.8	– 19.7 PT
nis-pg-bd-OH_2^+	–	– 6.3
Physisorption **pH = 4–9**		
dos-pg-OH_2^+-OH	0.0	– 144.8
dos-pg-OH_2^+-μOH	12.1	– 132.6
dos-pg-OH_2^+-$μ_3OH$	20.1	– 124.3
Chemisorption		
dis-pg-md-OH_2^+(μOH)	0.0	– 74.1
dis-pg-md-OH_2^+($μ_3OH$)	40.2	– 33.9
Physisorption **pH ~ 9**		
dos-ng-$μ_3OH$-$μ_3OH$	0.0	– 83.7
dos-ng-μOH-$μ_3OH$	9.6	– 74.1
dos-ng-OH-OH	25.5	– 58.2
dos-ng-μOH-μOH	28.0	– 55.6
dos-ng-OH-$μ_3OH$	33.1	– 50.6
dos-ng-OH-μOH	52.7	– 31.4
Physisorption **hypothetical**		
nos-ng-OH-OH → *dos-pg*-OH_2^+-$μ_3OH$	0.0	– 133.9 PT
nos-ng-OH-$μ_3OH$ → *dos-pg*-OH_2^+-$μ_3OH$	31.4	– 116.3 PT
nos-ng-OH-μOH → *dos-pg*-OH_2^+-μOH	35.6	– 103.8 PT
nos-ng-μOH-$μ_3OH$	72.4	– 72.8
nos-ng-μOH-μOH	75.7	– 69.9
nos-ng-μOH-OH	103.3	– 46.4
Chemisorption		
nis-ng-md-OH($μOH_{HB}$)—the same as		
dis-pg-md-OH($μOH_{HB}$)	0.0	– 32.6
nis-ng-md-μOH	14.6	– 18.0

Energies are in kJ/mol. Interaction energy is calculated according Eqs. 1–5. PT indicates proton transfer from neutral MCPA to goethite -OH site

[a]*nos* neutral MCPA, outer-sphere complex; *pg* protonated goethite—site OH_2^+; *dos* deprotonated MCPA, outer-sphere complex; *ng* neutral goethite surface; *nis* neutral inner-sphere complex; *md* monodentate complex; *dis* deprotonated inner-sphere complex

3.2 MCPA-goethite complexes at pH ~ 3–4

This section can be related to previous experimental data, revealing that the amount of adsorbed MCPA from aqueous solution increased with decreasing pH reaching the adsorption edge at pH_{50} ~ 4 [23].

3.2.1 Physisorbed outer-sphere hydrogen-bonded complexes of neutral MCPA with protonated goethite surface

In line of the acid–base properties of MCPA and goethite, neutral MCPA (nMCPA) and a protonated goethite (pG) surface can exist in solution at pH below 3–4. The protonation of the surface was done by adding a proton to one –OH group forming an $–OH_2^+$ site. To keep the overall neutral balance, one OH^- group was attached at the opposite side of the goethite model slab. The –COOH group of the neutral MCPA offers two sites for hydrogen bonding, which is carbonyl oxygen as a proton acceptor and carboxylic group as a proton donor. The goethite surface contains two sites that can act only as proton donors, which is the protonated $–OH_2^+$ site and the $–μ_3OH$ group, respectively. The rest –OH and –μOH groups can be proton donors and/or proton acceptors due to their flexibility.

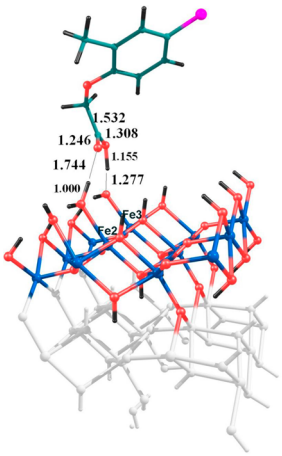

***nos-pg*-OH_2^+-OH**

Bond (Å)	
Fe-O_G	
Fe2-OH_2^+	2.23
Fe3-OH	2.07
Distance (Å)	
Fe-O_{MCPA}	
Fe2 - O_{carb}	4.50
Fe3 - O_{carb}	4.29
Fe2 - C_{carb}	5.37
Fe3 - C_{carb}	4.94

Fig. 2 Most stable physisorbed complex of neutral MCPA and protonated goethite surface ($FeOH_2^+$ site) reflecting pH bellow 4 (adsorption edge). O_G stands for the oxygen atom of goethite slab

Considering the structural features and distribution of the surface OH sites, two model complexes were selected—*nos-pg*-OH_2^+-OH (Fig. 2) and *nos-pg*-OH_2^+-μOH (Fig. S1 in Supplementary Material, SM). Used acronym ***nos-pg*** means ***neutral*** (MCPA) ***outer-sphere*** complex with ***protonated goethite*** surface. The most relevant geometric parameters (bond lengths and interatomic distances) of the optimized complexes are presented together with the figures. The formation of the physisorbed outer-sphere complex is written as:

$$\text{MCPA} + \text{G\_slab} \rightarrow \text{MCPA} \cdots \text{G\_slab} \quad (1)$$

Corresponding relative stabilities (ΔE_{rel}) and interaction energies (ΔE_{int}) are given in Table 2. The physisorption of the MCPA on the protonated goethite surface occurs through two hydrogen bonds, the $-C{=}O_{MCPA}\cdots H(OH^+)_G$ and $-OH_{MCPA}\cdots O_G$ (O_G from –OH or –μOH group). According to the energy calculations, the *nos-pg*-OH_2^+-OH complex is more stable than the *nos-pg*-OH_2^+-μOH by 13.8 kJ/mol (Table 2). The energy difference indicates that the surface complexation with $-OH_2^+$/–OH sites could be more probable, but this difference is small, and so the second type of the binding can be also possible. This hypothesis is also supported by the fact that both complexes have large interaction energies (− 81.2 kJ/mol vs. − 69.5 kJ/mol, Table 2). The large stabilization of the *nos-pg* complexes can be attributed mainly to quite strong hydrogen bonding between MCPA and surface OH sites (for the *nos-pg*-OH_2^+-OH complex, a very short $H_{MCPA}\cdots O(H)_G$ hydrogen bond of ~ 1.3 Å) and $O_{MCPA}\cdots H_2(O)_G$ hydrogen bond of ~ 1.7 Å) was detected, Fig. 2. The first hydrogen bonding observation corroborates the strong proton attractor properties of the surface –OH groups and the easy formation of $-OH_2^+$ surface sites. In the less stable *nos-pg* complex, the hydrogen $H_{MCPA}\cdots\mu O(H)_G$ bond of ~ 1.7 Å is weaker falling into the category of a medium-to-strong hydrogen bond [48]. Generally, in the goethite-MCPA complex, the surface Fe–O bond lengths increase in the order Fe-OH (2.07 Å, BO = 0.36) < Fe-μ_3OH (2.15 Å, BO = 0.31, both numbers are averaged values) ≈ Fe-μOH (2.14 Å, BO = 0.30, both numbers are averaged values) < Fe-OH_2 (~ 2.2–2.3 Å, BO ~ 0.25). Evidently, the Fe–O bond is weakened (BO decreases) with the increasing Fe–O distance. For comparison, the bond orders for bulk Fe–O and Fe-OH bonds are of ~ 0.5 and ~ 0.3, respectively, and they do not change upon MCPA adsorption. For six-coordinated Fe(III), its overall BO sum is about 2.5. The physisorption of the neutral MCPA molecule on the partially protonated goethite surface produces a slight elongation of the Fe-OH bond (~ 0.09 Å) due to $O(H)_G\cdots H_{MCPA}$ bonding. The protonation of the surface Fe-OH site to Fe-OH_2^+ resulted in relatively large elongation of the Fe–O bond by about 0.3 Å.

3.2.2 Chemisorbed inner-sphere complexes of neutral MCPA with protonated goethite surface

Two monodentate complexes, *nis-pg-md*-OH_2^+(OH) (Fig. 3) and *nis-pg-md*-OH_2^+(μOH), and one bidentate complex, *nis-pg-bd*-OH_2^+, were constructed and optimized (Fig. S2). ***Nis-pg-md*** means ***neutral inner-sphere*** complex with ***protonated goethite*** surface with ***monodentate binding*** and ***nis-pg-bd*** means ***neutral inner-sphere*** complex with ***protonated goethite*** and ***bidentate*** binding.

The formation of monodentate inner-sphere complexes (*nis-pg-md*-OH_2^+(OH) and *nis-pg-md*-OH_2^+(μOH)) and

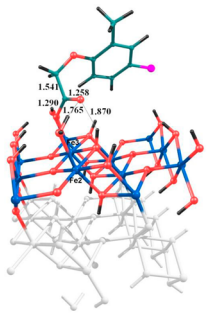

***nis-pg-md*-OH_2^+(OH_{HB})**
(proton transfer, O_{MCPA}-···H···OH_G)

Bond (Å)	
Fe-O_G	
Fe2 - OH_2^+ (HB)	2.202
Fe3 - O	2.223
Distance (Å)	
Fe-O_{MCPA}	
Fe3 - O_{carb}	2.248
Fe2 - O_{carb}	3.793
Fe3 - C_{carb}	3.200
Fe2 - C_{carb}	4.263

Fig. 3 Most stable chemisorbed complex of neutral MCPA and protonated goethite surface ($FeOH_2^+$ site), reflecting pH bellow 4 (adsorption edge). O_G stands for the oxygen atom of goethite slab and HB for hydrogen bond

the calculated interaction energy, ΔE_{int}, are obtained by an exchange reaction according Eq. 2:

$$G\left(OH_2^+\right) + HOOC-R \rightarrow GO(OH)C-R + H_2O \quad (2)$$

(G—goethite, MCPA = HOOC-R; R = $CH_2OC_6H_3ClCH_3$).

Formally, this formation reaction can be explained as a ligand replacement of the $-OH_2^+$ site (water molecule is released from the surface) with the carbonyl oxygen atom of the MCPA. As a result, one oxygen atom is shared by goethite and MCPA and forms a Fe–O–C bridge with Fe–O bond length of ~ 2.2 Å (BO ~ 0.26), being similar to the Fe-OH_2 distance in the physisorbed complex of neutral MCPA on the partially protonated goethite surface (Fig. 2, 2.23 Å, BO ~ 0.25) and a bit longer than a typical Fe–O bond in goethite (1.9–2.1 Å). The carboxylic OH group of MCPA was initially hydrogen bonded to the goethite proton acceptor atom (O) of the –OH or –μOH groups. During the optimization, the proton transfer from COOH to the corresponding goethite OH sites was observed forming protonated $-OH_2^+$ or $-\mu OH_2^+$ sites, respectively. In the optimized geometries of both complexes, the oxygen atom of the carboxyl group stayed in hydrogen bonding with the formed neighboring protonated sites after the proton transfer and with one neighboring μ_3OH (Figs. 3 and S2a). Owing to the protonation of Fe-OH, the Fe–O bond elongates by ~ 0.2 Å and its BO decreases from 0.41 to 0.26 being similar to the Fe-O_{MCPA} bond. All formed hydrogen bonds are of medium-to-strong strength in a range of 1.6–1.9. Very similar trends in changes of Fe–O bond lengths and bond orders upon protonation and MCPA adsorption have been found for all other complexes studied in this work and are not discussed further. The energy calculations of the monodentate complexes suggest much larger stabilization for the *nis-pg*-md-OH_2^+(OH) complex by 82.8 kJ/mol comparing to the *nis-pg-md*-OH_2^+(μOH), and also a large formation energy of − 102.5 kJ/mol. The significantly lower stabilization of the *nis-pg-md*-OH_2^+(μOH) complex indicates that its formation is less probable than the formation of the *nis-pg*-md-OH_2^+(OH) complex. The small interaction energy of − 19.7 kJ/mol can be attributed to the breaking of two Fe–O bonds by the replacement of the μOH group (Eq. 2). The protonation of μOH group and shorter $O_{MCPA}\cdots\mu H_2(O)_G$ bonds in *nis-pg-md*-OH_2^+(μOH) produces greater elongation (by 0.3 Å) of the related Fe-μO(H_2) bonds (Fig. S2a).

The topology of the OH surface sites allows formation of only one type of the bidentate complex; particularly, two neighboring –OH/$-OH_2^+$ groups are replaced by the MCPA, and two Fe–O–C bridges are formed by releasing of two H_2O molecules. The reaction energy of the *nis-pg-bd*-OH_2^+ complex formation (Fig. S2b) is calculated according to the exchange reaction by Eq. 3:

$$G\left(OHOH_2^+\right) + HOOC-R \rightarrow G(OOC-R) + 2H_2O \quad (3)$$

The calculated reaction energy is − 6.3 kJ/mol, formally showing an only slight stability of the bidentate complex. However, there is no experimental evidence that MCPA could be bound to the surface in a bidentate form. Possible explanation is that in such exchange reaction, two Fe–O bonds have to be broken, which can be a process with a high energetic barrier and thus not very likely due to kinetical hindrance. The measured Fe–O bond lengths in the bidentate chemisorbed complex were at 2.16–2.18 Å, slightly shorter than Fe–O bonds in the monodentate complexes. The O···O distance of two Fe–O–C bridges is ~ 2.28 Å, thus falling in a range of 2.27–2.29 Å typical for the carboxylic group.

The ΔE_{int} of *nis-pg-md*-OH_2^+(OH) is − 102.5 kJ/mol, which is larger by about 21 kJ/mol (in absolute value) than the interaction energy for the most stable physisorbed complex, *nos-pg*-OH_2^+-OH (− 81.2 kJ/mol). Hence, at pH = 3–4, the chemisorption mechanism with formation of inner-sphere complex on a bare surface (no solvent effect) can be predicted to be thermodynamically more favorable than the physisorbed complex. However, the formation of the inner-sphere complex requires a Fe–O bond breaking, which can be a reaction with the high energetic barrier; therefore, this could become a kinetically less favorable surface reaction than the formation of the outer-sphere complex. Previous studies have established that in aqueous solution, the affinity and basicity of a goethite surface can be reduced by the solvent effect, but at remaining of the activity trend of the adsorption sites [34]. The solvent effect can also have an impact on the interaction energies of both *nos-pg*-OH_2^+-OH (Fig. 2) and *nis-pg-md*-OH_2^+(OH) (Fig. 3). In general, we can conclude that both types of the MCPA surface complexation are probable and should be considered for the explanation of the experimental adsorption isotherm obtained in the acidic pH (3–5) range [23]. To approach the experiment and explain the increasing adsorption of MCPA with decreasing pH, these two MCPA-G complexes were solvated by explicitly adding a water slab (thickness of ~ 18 Å) and theoretically studied by molecular dynamics simulations. The results were reported in our previous work including slow motion animations of the surface structures formed during over 10 ps [23]. The MD simulations confirmed that the surface complexes can be partially destabilized by the solvent effect, but the overall configurations were preserved. The averaged geometrical parameters (e.g., Fe–O and C–O bond lengths) were successfully used in the CD-MUSIC modeling approach to interpret the experimentally observed dependence of the amount of MCPA adsorbed on pH [23].

3.3 MCPA-goethite complexes in pH range 4–9

The complexes of deprotonated MCPA (dMCPA) and partially protonated goethite (pG) surface were modeled to simulate the acid–base behavior of MCPA and goethite surface in a pH range 4–9. The MCPA carboxyl group is deprotonated in this pH range, whereas the –OH group of the goethite surface can attract a proton from solution.

3.3.1 Physisorbed outer-sphere hydrogen-bonded complexes of deprotonated MCPA with protonated goethite

The carboxylate group of dMCPA has two proton acceptor sites for hydrogen bonding. In total, three outer-sphere complexes were constructed, the *dos-pg*-OH_2^+-OH, the *dos-pg*-OH_2^+-μOH, and the *dos-pg*-OH_2^+-μ_3OH. In these configurations, the OH_2^+ group of the protonated goethite is a proton donor to one carboxylate oxygen, and the neighboring –OH, –μOH, or –μ_3OH groups served as a proton donor to the second carboxylate oxygen of dMCPA. The acronym ***dos-pg*** means ***deprotonated outer-sphere*** complex with ***protonated goethite***. The calculation of the interaction energies predicted that the *dos-pg*-OH_2^+-OH complex (Fig. 4) is the most stable comparing to the other two configurations (Table 2), with a relatively large interaction energy ΔE_{int} of − 144.8 kJ/mol. The interaction occurs mainly by formation of (1) two hydrogen bonds between one carboxylate oxygen and protons of –OH_2^+ group (1.636 Å) and –μ_3OH (1.843 Å), (2) one hydrogen bond between the second carboxylate oxygen and –OH group (1.712 Å), and (3) weaker Cl···μOH hydrogen bond (2.301 Å). The other two complexes (*dos-pg*-OH_2^+-μOH and *dos-pg*-OH_2^+-μ_3OH, Fig. S3) are only slightly higher in energy by 12.2 and 20.5 kJ/mol, respectively. Thus, all three possible surface complexes do not differ much by their calculated stability. As to be expected, the interaction energies between charged MCPA and protonated goethite surface are larger than interaction energies of neutral MCPA and protonated goethite (Table 2). The strong physisorption for the bare dMCPA-pG complexes thus predicted is not supported by the experimental adsorption edge showing a decrease in MCPA adsorption with pH increase [23]. The reason for this discrepancy is the strong destabilization role of solvent effect on the physisorbed dMCPA-pG complexes. The solvation energy calculated for the neutral MCPA is − 59.4 kJ/mol, whereas for the MCPA anion accounts for as high as − 304.2 kJ/mol (obtained with the Turbomole program [49], PBE functional, TZVP basis set [50], and the COSMO model for water solvent [51]). The presence of the strong polar solvent effect would disrupt hydrogen bonding of the outer-sphere complexes because of the high solvent energy of the MCPA anion. In addition, the hydration of the hydroxylated goethite surface can also contribute to the destabilization of the dMCPA-pG complexes at pH 4–9. Thus, these two effects can explain why the MCPA adsorption decreases with increasing pH. Similar trends have been found for adsorption of other phenoxyacetic herbicides on clay minerals [7, 16].

3.3.2 Chemisorbed inner-sphere complexes of deprotonated MCPA with protonated goethite

Two monodentate complexes were constructed, which are the *dis-pg-md*-OH_2^+(μOH) (Fig. 5) and *dis-pg-md*-OH_2^+(μ_3OH) (Fig. S4). Acronym ***dis-pg-md*** means ***deprotonated inner-sphere*** complex with ***protonated goethite*** in ***monodentate*** binding by the Fe–O-C bridge. Formally, the interaction reaction can be described by Eq. 4, in which one H_2O molecule is released:

$$G\left(OH_2^+\right) + OOC-R^- \rightarrow G(OOCR) + H_2O \quad (4)$$

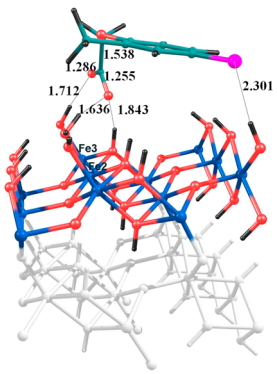

Bond (Å)	
Fe-O_G	
Fe2-OH_2^+ (HB)	2.113
Fe3-OH (HB)	2.179
Distance (Å)	
Fe-O_{MCPA}	
Fe2 - O_{carb}	3.550
Fe3 - O_{carb}	4.035
Fe2 - C_{carb}	4.624
Fe3 - C_{carb}	4.457

dos-pg-OH_2^+-OH

Fig. 4 Most stable physisorbed complex of deprotonated MCPA and protonated goethite surface ($FeOH_2^+$), reflecting pH range 4–9

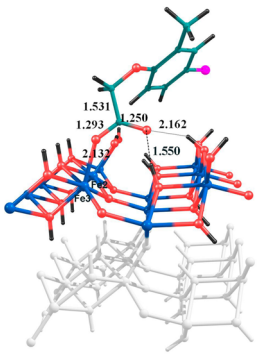

Bond (Å)	
Fe-O	
Fe3 – O_{carb}	2.132
Fe3-μ_3O	1.952
Fe3-μ_3O	1.945
Fe3-μ_3OH	2.115
Fe3-μ_3OH	2.111
Fe3-μ_3OH	2.093
Distance (Å)	
Fe-O_{MCPA}	
Fe3 - $O_{carb\ (free)}$	3.696
Fe3 - C_{carb}	3.216
Fe2 - C_{carb}	4.173

dis-pg-md-OH_2^+(μ_3OH_{HB}, μOH_{HB})

Fig. 5 Most stable chemisorbed complex of deprotonated MCPA and protonated goethite surface ($FeOH_2^+$ site), reflecting pH range 4–9

The second carboxylate O atom is involved in hydrogen bonding with proton donor atoms of $–\mu_3OH$ or –μOH groups depending on the orientation of MCPA on the surface. A larger stability (by 40.2 kJ/mol) and larger interaction energy (− 74.1 kJ/mol) were found for the *dis*-pg-md-OH_2^+(μOH) complex (Table 2) due to two hydrogen bonds formed by free carbonyl O with $–\mu_3OH$ and –μOH groups, respectively. Moreover, the Fe–O(C) bond is shorter in the more stable complex (2.132 Å *vs.* 2.208 Å, Figs. 5 and S4). The calculated interaction energy of the most stable bare outer-sphere complex (− 144.8 kJ/mol, Table 2) is larger than that of the inner-sphere complex (− 74.1 kJ/mol). Therefore, the physisorption of MCPA to goethite at pH 4–9 would be hypothetically preferred in the absence of a polar solvent phase. In case of polar solution present, however, the outer-sphere complex will be strongly destabilized due to a high solvation energy of the MCPA anion. The inner-sphere complex of the MCPA anion, *dis-pg-md*-OH(μOH), resembles the inner-sphere complex of neutral MCPA, *nis-pg-md*-OH_2^+(OH), since in the latter a spontaneous proton transfer and MCPA deprotonation was observed. Hence, it is expected that the solvent effect on the inner-dMCPA-pG complex is similar to that of the nMCPA-pG complex. This leads to a small elongation of Fe–O and C–O bonds and perturbation of hydrogen bonds between free O_{carb} with the neighboring OH groups. If outer-sphere complexes are strongly disrupted by the solvation of the MCPA anion at pH > 4, the inner-sphere dMCPA-pG complex can still exist and could explain why the goethite surface has still some adsorption capacity for MCPA at a pH range 4–9 [23].

3.4 MCPA-goethite complexes at pH ~ 9

3.4.1 Physisorbed outer-sphere hydrogen-bonded complexes of deprotonated MCPA with neutral goethite surface

In the alkaline pH range, the goethite surface becomes neutral or even deprotonated. For the (net) neutral goethite surface, the –OH and –μOH groups can act as a proton donor and/or acceptor, respectively, while the $–\mu_3OH$ group can become a proton donor only. Six complexes can be formed for this situation, which are the *dos-ng*-μ_3OH-μ_3OH (Fig. 6), the *dos-ng*-μOH-μ_3OH, the *dos-ng*-OH-OH, the *dos-ng*-μOH-μOH, the *dos-ng*-OH-μ_3OH, and the *dos-ng*-OH-μOH (Fig. S5). Acronym ***dos-ng*** means ***deprotonated outer-sphere*** complex with ***neutral goethite***. To keep the overall neutrality of the models in the calculations, we added one proton to one –OH group at the opposite side of the goethite model slab. In this case, the physisorption mechanism is also represented by hydrogen bonding between MCPA and the surface OH groups. Apart from previously discussed physisorbed complexes at lower pH, the most stable complex

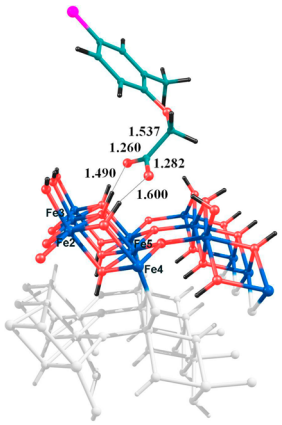

***dos-ng*-μ_3OH-μ_3OH**

Bond (Å)	
Fe-O_G	
Fe3-μ_3OH (HB)	2.093
Fe2-μ_3OH (HB)	2.089
Fe2-μ_3OH (HB)	2.075
Fe5-μ_3OH (HB)	2.090
Fe4-μ_3OH (HB)	2.084
Distance (Å)	
Fe-O_{MCPA}	
Fe5 - O_{carb}	3.890
Fe2 - O_{carb}	4.071
Fe4 - O_{carb}	3.562
Fe3 - O_{carb}	4.135
Fe2 - C_{carb}	4.335
Fe4 - C_{carb}	4.443
Fe5 - C_{carb}	4.368
Fe3 - C_{carb}	5.234

Fig. 6 Most stable physisorbed complex of deprotonated MCPA and neutral goethite surface at pH ~ 9

was found for the configuration, in which two carboxylate oxygen atoms are acting as proton acceptors for two neighboring $–\mu_3OH$ groups (d*os-ng*-μ_3OH-μ_3OH, Table 2, Fig. 6). The stabilization effect is relatively high, comparable with that of the physisorbed complex of neutral MCPA at the protonated surface (*nos-pg*-OH_2^+(OH), Fig. 2). Other possible configurations representing different combinations of –OH, –μOH, and $–\mu_3OH$ in the hydrogen bonding (Table 2) are less stable by about 10–52 kJ/mol. In the energetically most stable complex, two relatively strong $O_{carb}\cdots H(\mu_3OH)$ hydrogen bonds were formed (1.490 Å and 1.600 Å).

3.5 MCPA-goethite complexes of neutral MCPA molecule on neutral goethite surface (hypothetical)

To complete all possible combinations, we performed also calculations on interactions of neutral MCPA molecule with the neutral goethite surface. In principle, this combination is only hypothetical with respect to acid–base properties of MCPA and the goethite surface (i.e., such a configuration cannot coexist simultaneously in any pH range).

3.5.1 Physisorbed outer-sphere hydrogen-bonded complexes of neutral MCPA with neutral goethite surface

In total, six different initial configurations have been optimized. Possible combinations of hydrogen bonds between the –COOH group and the surface –OH groups of goethite were modeled respecting the OH topology and taking into account that –COOH and –OH/μOH groups possess proton donor or acceptor capabilities, whereas μ_3OH can act only as a proton donor [19, 34]. The models built were

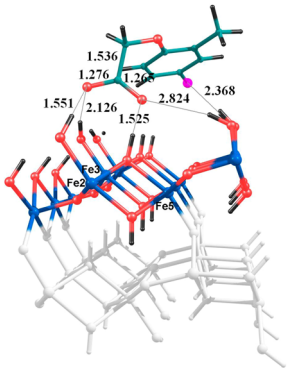

Bond (Å)	
Fe-O_G	
Fe2-OH_2^+ (HB)	2.140
Fe3-OH (HB)	1.952
Distance (Å)	
Fe-O_{MCPA}	
Fe2 - O_{carb}	4.018
Fe2 - O_{carb}	4.048
Fe3 - O_{carb}	4.179
Fe3 - O_{carb}	4.005
Fe3 - C_{carb}	4.405
Fe2 - C_{carb}	4.428

***nos-ng*-OH-OH**
(proton transfer and change to *dos-pg*-OH_2^+-μ_3OH)

Fig. 7 Most stable (hypothetical) physisorbed complex of neutral MCPA on neutral goethite surface (pH range 4–9)

nos-ng-OH-OH (Fig. 7), *nos-ng*-OH-μ_3OH, *nos-ng*-OH-μOH, *nos-ng*-μOH-μ_3OH, *nos-ng*-μOH-μOH, and *nos-ng*-μOH-OH (Fig. S6). Acronym ***nos-ng*** means ***neutral outer-sphere*** complex with ***neutral goethite***.

The first three outer-sphere complexes (*nos-ng*-OH-OH, *nos-ng*-OH-μ_3OH, and *nos-ng*-OH-μOH) are more stable configurations than the remaining three (Table 2). The dominant interaction in the three physisorbed complexes is the Fe(H)O···HOOC bonding, which during the optimization transforms to a Fe(H)OH^+···OOC^- complex because of a proton transfer from the carboxyl group to the surface –OH group. The formation of the positively charged surface site –Fe-OH_2^+ demonstrates its high stability and a strong proton affinity character of the hydroxo groups of goethite, being in line with the calculated proton binding constant pK_a for –OH groups [34]. Moreover, during the optimization, the geometry of the *nos-ng*-OH-OH complex changed to the *dos-pg*-OH_2^+-μ_3OH complex (Fig. 7) with the largest interaction energy of − 133.9 kJ/mol. This complex is stabilized by two strong hydrogen bonds (1.551 Å and 1.525 Å) between the two carboxylate oxygen atoms and the proton donor groups –OH_2^+ and –μ_3OH, respectively. Moreover, the carboxylate group enables to form additional hydrogen bonds with OH groups (Fe-OH and Fe-μOH) in vicinity of the interacting site. In addition, the Cl atom of the MCPA molecule forms a weak hydrogen bonding with another Fe-μOH group enhancing the physisorption of MCPA to goethite. After the proton transfer, the MCPA-goethite complex can be regarded as an outer-sphere complex formed between MCPA anion and partially protonated goethite surface *(dos-pg* interaction type). The observed proton transfer as appeared also for two other stable MCPA-goethite complexes (Table 2) indicates a strong proton affinity of the –OH group and formation of real outer-sphere complexes between the MCPA anion and a goethite surface (partially) protonated in the pH 4–9 range as described in Sect. 3.3.1.

3.5.2 Chemisorbed inner-sphere monodentate complexes of neutral MCPA with neutral goethite surface

In these complexes, one surface OH group was replaced by formation of a Fe–O–C bridge. This reaction is accompanied by the release of one water molecule (Eq. 5). Two possible structures were taken into the account, in which surface –OH and –μOH groups were removed. The models were labeled as monodentate *nis-ng-md*-OH(μOH)) and *nis-ng-md*-μOH (Fig. S7) complexes:

$$G(OH/\mu OH) + HOOCR \rightarrow G(OOCR) + H_2O \quad (5)$$

The acronym ***nis-ng-md*** means ***neutral inner-sphere*** complex with ***neutral goethite monodentate*** binding. The *nis-ng-md*-OH(μOH) complex was found as more stable chemisorbed inner-sphere complex compared to the second complex, *nis-ng-md*-μOH (Table 2). In fact, this complex is the same as the *dis-pg-md*-OH(μOH) complex already discussed in Sect. 3.3.2 (Fig. 5).

4 Conclusions

In this work, we used the DFT method in the study of the formation mechanisms of surface complexes between the MCPA herbicide and the predominant (110) surface of the mineral goethite. Our simulations reflected the strong pH effect on MCPA adsorption by including the anionic form of MCPA and the protonated goethite surface into the calculations. To include such pH effects in DFT modeling is by far not trivial and common. Different types of the surface OH groups, their topology at the surface, the structure of carboxyl/carboxylate group of MCPA, offered a plenty of possible combinations for MCPA binding to the goethite surface. Moreover, from the possible surface complexation mechanisms, both outer- (physisorbed) and inner-sphere (chemisorbed) complexes were modeled. The stability of complexes was evaluated on the base of the relative and interaction energies. Acid–base properties of MCPA and the goethite surface OH groups led to creation of several pH ranges for the different neutral/deprotonated MCPA with neutral/protonated goethite surface combinations possible.

The calculations showed that the basic mechanism for the formation of the outer-sphere complexes is the formation of hydrogen bonds of a different strength, depending on which moiety is proton donor or acceptor, respectively. It was shown that among the three types of the surface OH groups, the most active is the –OH group bound to one Fe atom. This group can easily attract a proton from aqueous solution and

is responsible for the positively charged goethite surface at circumneutral to acidic pH values. Although in the pH range 4–9, the most stable physisorbed complexes were found for the MCPA anion adsorbed on the protonated goethite surface (with an interaction energy in a range of − 124 to − 145 kJ/mol), their stability in reality would be strongly reduced due to the large solvation energy of the MCPA anion. For the pH values close to the pK_a value of MCPA, the neutral MCPA molecule interacts weaker with the protonated goethite surface (interaction energy of about − 80 kJ/mol); however, the outer-sphere complex potentially formed can be more stable in the solution than the complex of MCPA anion because of the much lower solvation energy of the neutral MCPA. Thus, adsorption of MCPA should increase with decreasing pH. This conclusion is in agreement with the experimental observations reported earlier, in which the highest adsorbed amount was achieved for the pH ~ 3.

In the chemisorbed inner-sphere complexes, monodentate binding was formed through the Fe–O–C bridge. The protonated surface –OH group (–OH_2^+ site) represents a key in the exchange reaction, in which one water molecule is released to solution and replaced by the carboxyl/carboxylate group of the MCPA moiety. We have found that at low pH (~ 3), the chemisorbed monodentate MCPA-goethite complex has larger adsorption energy (in absolute value) than other chemisorbed complexes formed at higher pH values. In addition, this energy is also higher (in absolute value) than the adsorption energy of the outer-sphere complex at pH ~ 3 by about 21 kJ/mol, which proves that the formation of the inner-sphere complex at low pH can significantly contribute to the overall adsorption of MCPA.

Acknowledgements We are grateful for the financial support the German Research Foundation (No. GE 1676/1) of priority research program SPP 1315. I.G thanks for the financial support the Bulgarian National Science Fund of Bulgarian Ministry of Education and Science, Grant DH09/9/2016. The authors also acknowledge the technical support and computer time at the Vienna Scientific Computing (VSC) cluster.

References

1. Walker M, Lawrence H (1992) EPA's pesticide fact sheet database. Lewis Publishers Inc., Chelsea
2. Haberhauer G, Pfeiffer L, Gerzabek MH (2000) Influence of molecular structure on sorption of phenoxyalkanoic herbicides on soil and its particle size fractions. J Agric Food Chem 48(8):3722–3727. https://doi.org/10.1021/jf9912856
3. Haberhauer G, Pfeiffer L, Gerzabek MH, Kirchmann H, Aquino AJA, Tunega D, Lischka H (2001) Response of sorption processes of MCPA to the amount and origin of organic matter in a long-term field experiment. Eur J Soil Sci 52(2):279–286. https://doi.org/10.1046/j.1365-2389.2001.00382.x
4. Socias-Viciana MH, Fernandez-Perez M, Villafranca-Sanchez R, Gonzalez-Pradas E, Flores-Cespedes F (1999) Sorption and leaching of atrazine and MCPA in natural and peat-amended calcareous soils from Spain. J Agric Food Chem 47(3):1236–1241. https://doi.org/10.1021/jf980799m
5. Clausen L, Fabricius I (2001) Atrazine, isoproturon, mecoprop, 2,4-D, and bentazone adsorption onto iron oxides. J Environ Qual 30(3):858–869. https://doi.org/10.2134/jeq2001.303858x
6. Inacio J, Taviot-Gueho C, Forano C, Besse JP (2001) Adsorption of MCPA pesticide by MgAl-layered double hydroxides. Appl Clay Sci 18(5–6):255–264. https://doi.org/10.1016/s0169-1317(01)00029-1
7. Vasudevan D, Cooper EM, Van Exem OL (2002) Sorption-desorption of lonogenic compounds at the mineral-water interface: study of metal oxide-rich soils and pure-phase minerals. Environ Sci Technol 36(3):501–511. https://doi.org/10.1021/Es0109390
8. Thorstensen CW, Lode O (2001) Laboratory degradation studies of bentazone, dichlorprop, MCPA, and propiconazole in Norwegian soils. J Environ Qual 30(3):947–953. https://doi.org/10.2134/jeq2001.303947x
9. Pignatello JJ, Xing BS (1996) Mechanisms of slow sorption of organic chemicals to natural particles. Environ Sci Technol 30(1):1–11. https://doi.org/10.1021/Es940683g
10. Benoit P, Barriuso E, Calvet R (1998) Biosorption characterization of herbicides, 2,4-D and atrazine, and two chlorophenols on fungal mycelium. Chemosphere 37(7):1271–1282. https://doi.org/10.1016/S0045-6535(98)00125-8
11. Bolan NS, Baskaran S (1996) Biodegradation of 2,4-D herbicide as affected by its adsorption–desorption behaviour and microbial activity of soils. Aust J Soil Res 34(6):1041–1053. https://doi.org/10.1071/Sr9961041
12. DePaolis F, Kukkonen J (1997) Binding of organic pollutants to humic and fulvic acids: Influence of pH and the structure of humic material. Chemosphere 34(8):1693–1704. https://doi.org/10.1016/S0045-6535(97)00026-X
13. Sannino F, Violante A, Gianfreda L (1997) Adsorption-desorption of 2,4-D by hydroxy aluminium montmorillonite complexes. Pestic Sci 51(4):429–435. https://doi.org/10.1002/(sici)1096-9063(199712)51:4<429:aid-ps619>3.0.co;2-j
14. Susarla S, Bhaskar GV, Bhamidimarri SMR (1997) Competitive adsorption-desorption kinetics of phenoxyacetic acids and a chlorophenol in volcanic soil. Environ Technol 18(9):937–943. https://doi.org/10.1080/09593331808616613
15. Celis R, Hermosin MC, Cox L, Cornejo J (1999) Sorption of 2,4-dichlorophenoxyacetic acid by model particles simulating naturally occurring soil colloids. Environ Sci Technol 33(8):1200–1206. https://doi.org/10.1021/es980659t
16. Cox L, Celis R, Hermosin MC, Cornejo J (2000) Natural soil colloids to retard simazine and 2,4-d leaching in soil. J Agric Food Chem 48(1):93–99. https://doi.org/10.1021/Jf990585k
17. Spadotto CA, Hornsby AG (2003) Soil sorption of acidic pesticides: modeling pH effects. J Environ Qual 32(3):949–956. https://doi.org/10.2134/jeq2003.9490
18. Jensen PH, Hansen HCB, Rasmussen J, Jacobsen OS (2004) Sorption-controlled degradation kinetics of MCPA in soil. Environ Sci Technol 38(24):6662–6668. https://doi.org/10.1021/Es0494095
19. Aquino AJA, Tunega D, Haberhauer G, Gerzabek MH, Lischka H (2007) Quantum chemical adsorption studies on the (110) surface of the mineral goethite. J Phys Chem C 111(2):877–885. https://doi.org/10.1021/Jp0649192
20. Tunega D, Gerzabek MH, Haberhauer G, Totsche KU, Lischka H (2009) Model study on sorption of polycyclic aromatic hydrocarbons to goethite. J Colloid Interface Sci 330(1):244–249. https://doi.org/10.1016/j.jcis.2008.10.056
21. Tunega D, Haberhauer G, Gerzabek MH, Lischka H (2004) Sorption of phenoxyacetic acid herbicides on the kaolinite mineral surface—an ab initio molecular dynamics simulation. Soil Sci 169(1):44–54. https://doi.org/10.1097/01.ss.0000112015.97541.f3

22. Tunega D, Gerzabek MH, Haberhauer G, Lischka H (2007) Formation of 2,4-D complexes on montmorillonites—an ab initio molecular dynamics study. Eur J Soil Sci 58(3):680–691. https://doi.org/10.1111/j.1365-2389.2006.00853
23. Kersten M, Tunega D, Georgieva I, Vlasova N, Branscheid R (2014) Adsorption of the herbicide 4-chloro-2-methylphenoxyacetic acid (MCPA) by goethite. Environ Sci Technol 48(20):11803–11810. https://doi.org/10.1021/Es502444c
24. Werner D, Garratt JA, Pigott G (2013) Sorption of 2,4-D and other phenoxy herbicides to soil, organic matter, and minerals. J Soil Sediment 13(1):129–139. https://doi.org/10.1007/s11368-012-0589-7
25. Pronk GJ, Heister K, Kogel-Knabner I (2011) Iron oxides as major available interface component in loamy arable topsoils. Soil Sci Soc Am J 75(6):2158–2168. https://doi.org/10.2136/sssaj2010.0455
26. Iglesias A, Lopez R, Gondar D, Antelo J, Fiol S, Arce F (2010) Adsorption of MCPA on goethite and humic acid-coated goethite. Chemosphere 78(11):1403–1408. https://doi.org/10.1016/j.chemosphere.2009.12.063
27. Angove MJ, Fernandes MB, Ikhsan J (2002) The sorption of anthracene onto goethite and kaolinite in the presence of some benzene carboxylic acids. J Colloid Interface Sci 247(2):282–289. https://doi.org/10.1006/jcis.2001.8133
28. Muller S, Totsche KU, Kogel-Knabner I (2007) Sorption of polycyclic aromatic hydrocarbons to mineral surfaces. Eur J Soil Sci 58(4):918–931. https://doi.org/10.1111/j.1365-2389.2007.00930.x
29. Weigand H, Totsche KU (1998) Flow and reactivity effects on dissolved organic matter transport in soil columns. Soil Sci Soc Am J 62(5):1268–1274. https://doi.org/10.2136/sssaj1998.03615995006200050017x
30. Gaboriaud F, Ehrhardt J (2003) Effects of different crystal faces on the surface charge of colloidal goethite (alpha-FeOOH) particles: an experimental and modeling study. Geochim Cosmochim Ac 67(5):967–983. https://doi.org/10.1016/S0016-7037(02)00988-2
31. Kavanagh BV, Posner AM, Quirk JP (1977) Adsorption of phenoxyacetic acid herbicides on goethite. J Colloid Interface Sci 61(3):545–553. https://doi.org/10.1016/0021-9797(77)90472-6
32. Iglesias A, Lopez R, Gondar D, Antelo J, Fiol S, Arce F (2009) Effect of pH and ionic strength on the binding of paraquat and MCPA by soil fulvic and humic acids. Chemosphere 76(1):107–113. https://doi.org/10.1016/j.chemosphere.2009.02.012
33. Boily JF, Persson P, Sjoberg S (2000) Benzenecarboxylate surface complexation at the goethite (alpha-FeOOH)/water interface: II. Linking IR spectroscopic observations to mechanistic surface complexation models for phthalate, trimellitate, and pyromellitate. Geochim Cosmochim Acta 64(20):3453–3470. https://doi.org/10.1016/S0016-7037(00)00453-1
34. Aquino AJA, Tunega D, Haberhauer G, Gerzabek MH, Lischka H (2008) Acid–base properties of a goethite surface model: a theoretical view. Geochim Cosmochim Acta 72(15):3587–3602. https://doi.org/10.1016/j.gca.2008.04.037
35. Kresse G, Furthmuller J (1996) Efficient iterative schemes for ab initio total-energy calculations using a plane-wave basis set. Phys Rev B 54(16):11169–11186. https://doi.org/10.1103/physrevb.54.11169
36. Perdew JP, Burke K, Ernzerhof M (1996) Generalized gradient approximation made simple. Phys Rev Lett 77(18):3865–3868. https://doi.org/10.1103/physrevlett.77.3865
37. Kresse G, Joubert D (1999) From ultrasoft pseudopotentials to the projector augmented-wave method. Phys Rev B 59(3):1758–1775. https://doi.org/10.1103/PhysRevB.59.1758
38. Dudarev SL, Botton GA, Savrasov SY, Humphreys CJ, Sutton AP (1998) Electron-energy-loss spectra and the structural stability of nickel oxide: an LSDA+U study. Phys Rev B 57(3):1505–1509. https://doi.org/10.1103/PhysRevB.57.1505
39. Otte K, Pentcheva R, Schmahl WW, Rustad JR (2009) Pressure-induced structural and electronic transitions in FeOOH from first principles. Phys Rev B. https://doi.org/10.1103/Physrevb.80.205116
40. Tunega D (2012) Theoretical study of properties of goethite (alpha-FeOOH) at ambient and high-pressure conditions. J Phys Chem C 116(11):6703–6713. https://doi.org/10.1021/Jp2091297
41. Hazemann JL, Berar JF, Manceau A (1991) Rietveld studies of the aluminum-iron substitution in synthetic goethite. Mater Sci Forum 79:821–826. https://doi.org/10.4028/www.scientific.net/MSF.79-82.821
42. Bucko T, Hafner J, Angyan JG (2005) Geometry optimization of periodic systems using internal coordinates. J Chem Phys. https://doi.org/10.1063/1.1864932
43. Baker J, Kessi A, Delley B (1996) The generation and use of delocalized internal coordinates in geometry optimization. J Chem Phys 105(1):192–212. https://doi.org/10.1063/1.471864
44. Manz TA, Limas NG (2016) Introducing DDEC6 atomic population analysis: part 1. Charge partitioning theory and methodology. RSC Adv 6(53):47771–47801. https://doi.org/10.1039/C6RA04656H
45. Manz T, Limas NG (2017) Chargemol program for performing DDEC analysis. https://ddec.sourceforge.net/. Accessed Aug 2017.
46. Manz TA (2017) Introducing DDEC6 atomic population analysis: part 3. Comprehensive method to compute bond orders. RSC Adv 7(72):45552–45581. https://doi.org/10.1039/c7ra07400j
47. Manz TA, Yang B (2016) Selective oxidation passing through eta(3)-ozone intermediates: applications to direct propene epoxidation using molecular oxygen oxidant (vol 4, pg 27755, 2014). RSC Adv 6(110):108153. https://doi.org/10.1039/C4RA03729D
48. Desiraju GR, Steiner T (2001) The weak hydrogen bond in structural chemistry and biology. OUP, Chichester
49. Ahlrichs R, Bar M, Haser M, Horn H, Kolmel C (1989) Electronic-structure calculations on workstation computers—the program system turbomole. Chem Phys Lett 162(3):165–169. https://doi.org/10.1016/0009-2614(89)85118-8
50. Schafer A, Huber C, Ahlrichs R (1994) Fully optimized contracted gaussian-basis sets of triple zeta valence quality for atoms Li to Kr. J Chem Phys 100(8):5829–5835. https://doi.org/10.1063/1.467146
51. Klamt A, Schuurmann G (1993) Cosmo—a new approach to dielectric screening in solvents with explicit expressions for the screening energy and its gradient. J Chem Soc Perk T 2(5):799–805. https://doi.org/10.1039/P29930000799